2nd International Conference on Ultrafine Grained &
Nanostructured Materials (UFGNSM)
International Journal of Modern Physics: Conference Series
Vol. 5 (2012) 325–334

DOI: 10.1142/S201019451200219X

World Scientific
www.worldscientific.com

DEVELOPMENT OF CRYSTALLOGRAPHIC TEXTURE AND GRAIN REFINEMENT IN THE ALUMINUM LAYER OF CU-AL-CU TRI-LAYER COMPOSITE DEFORMED BY EQUAL CHANNEL ANGULAR EXTRUSION

B.TOLAMINEJAD

School of Metallurgy and Materials Engineering, Iran University of Science and Technology, Narmak, Tehran, Iran
btolaminejad@iust.ac.ir

A.KARIMI TAHERI, M.SHAHMIRI, H.ARABI

Department of Materials Science and Engineering, Sharif University of Technology, Azadi Ave, Tehran, Iran
School of Metallurgy and Materials Engineering, Iran University of Science and Technology, Narmak, Tehran, Iran
ktaheri@sharif.edu, mshahmiri@iust.ac.ir, arabi@iust.ac.ir

The present research is concerned with the aluminum layer of a loosely packed tri-layer copper-aluminum-copper composite deformed by ECAE process. Electron back scattered diffraction (EBSD), transmission electron microscope, and X-ray technique were employed to investigate the detailed changes occurring in the microtexture, microstructure (cell size and misorientation), and dislocation density evolution during consecutive passes of ECAE process performed on the composite based on route Bc. According to tensile test results, the yield stress of the aluminum layer was increased significantly after application of ECAE throughout the four repeated passes and then slightly decreased. An ultrafine grain size within the range of 500-600 nm was obtained in the Al layer by increasing the thickness of copper layers. It was observed that the reduction of grain size in the aluminum layer is nearly 57% more than that of an ECAE-ed single layer aluminum billet. Also, the grain refinement of the aluminum layer is accelerated throughout 8 passes. This observation was attributed to the higher rate of dislocation interaction, cell formation and texture development during the ECAE of the composite compared to those of the single billet.

Keywords: ECAE; copper-aluminum-copper; texture; laminated composite; ultrafine grain.

1. Introduction

During the past several decades, extensive researches have been carried out in the field of materials science and manufacturing engineering to produce materials of high performance capabilities and fabrication cost efficiency. A dramatic improvement has been achieved when dissimilar materials are combined to form composites of various natures. Among the composite materials, the laminated ones are used in various industries. For instance, it has been reported that there are many advantages of copper

clad aluminum (CCA) for electric and electronic applications. It is 30-40% cheaper and 60% lighter than the conventional copper product including DHP, DLP and PFCH.[1] Usually, the laminated composites are fabricated by solid state joining techniques, such as diffusion bonding[2], friction stir welding[3], extrusion[1], and roll bonding.[4] On the other hand, in recent years research on the severe plastic deformation (SPD) processing, structure and mechanical behavior of nanocrystalline (d<100 nm) and ultrafine grained (100nm<d<1μm) materials has thrived.[5] As a SPD process, equal channel angular extrusion (ECAE) has been developed and passed from the laboratory stage to industrial condition.[6] Fig. 1 shows the schematic of ECAE die consisting of a die angle (φ) and an outer curved corner angle (ψ). The die initially is charged with a billet inserted in the vertical channel and then pushed into the horizontal channel with the aid of a punch. Under this condition a large shear strain is induced in the billet, while the cross section of the billet does not experience any change. Eq. (1) presents the equivalent strain imposed on the billet after N passes of ECAE [7]:

$$\bar{\varepsilon}_N = \frac{N}{\sqrt{3}}\left(2\cot\left(\frac{\phi+\psi}{2}\right)+\psi\,\mathrm{cosec}\left(\frac{\phi+\psi}{2}\right)\right) \tag{1}$$

In this research a new application of the ECAE process which is deformation of bimetallic clad strips, introduced by Eivani et al.[8], is developed with a view to microstructural and textural evolution. The motivation for this work arose from the effect of cladding on the deformation of middle layer of a tri-layer strip. It was assumed that

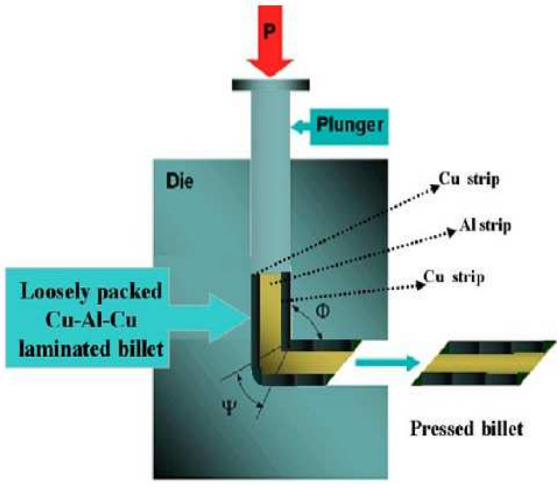

Fig. 1. The schematic of equal channel angular extrusion of loosely packed Cu-Al-Cu billet.

different operative slip systems may be affected on a microscopic level leading to a different texture and further grain refinement. To assess the hypothesis, an aluminum strip is sandwiched between two hard strips of commercial pure copper. Then, such a loosely packed Cu-Al-Cu laminated billet is deformed by several passes of ECAE process as shown schematically in Fig. 1. The aim is to produce an ultrafine grain structure of mean grain size of much smaller than 1300 nm and in a smaller number of ECAE pass (less than 8 passes) used so far for a commercial pure aluminum strip.[9]

2. Experimental Procedure

The materials used in this research consisted of commercial pure aluminum (A1070-P-H12) and copper (C 1201 P) strips and commercial pure aluminum rod. Aluminum strips had dimensions of either 70×14×5 mm or 70×14×9 mm. The copper strips had a length of 70 mm, width of 14 mm, and thickness of either 2.5 or 4.5 mm. The rod was machined to produce a single aluminum billet. The dimensions of aluminum billet used as the proof specimen were 70×14×14 mm. All of the strips and the Al billet were annealed at 400^{o}C for 30 min before subjecting them to ECAE process. To promote the joining between the strips during co-extrusion, a surface preparation process was carried out for each strip prior to ECAE operation. Then, the Al strip was sandwiched between the Cu strips to present a loosely packed Cu-Al-Cu laminated composite billet. The composite having Cu layer with a thickness of 2.5 mm was coded as type I composite and the one having Cu layer of 4.5 mm thickness hereinafter named type II. In order to perform the ECAE tests, a split die with an inner angle of φ=90^{o}, outer corner angle of ψ=20^{o}, and a square cross section of 14×14mm was made. ECAE tests via route Bc (90^{o} clockwise rotation of the specimen after each pass)[10] were carried out on the composite as well as the aluminum billet at room temperature under a constant press velocity of 3 mm/s by means of a hydraulic press. The tests were carried out up to 8 passes using MoS_2 spray as the lubricant. To study the microstructure of the aluminum layer in the composite and that of the aluminum billet after being subjected to different number of passes, specimens with dimensions of 12×4×2 mm were cut from the ECAE-ed aluminum billet and the aluminum layer located at the middle of ECAE-ed laminated billet. Then, some sections of aluminum layer parallel to the deformed flow plane were cut from the center of these specimens to study their microstructures. Standard tensile test specimens were machined from the deformed aluminum billet and the aluminum layer according to ASTM E-8. These specimens were subjected to tensile test at a strain rate of $2\times10^{-3}s^{-1}$ using the Instron tensile testing machine model 5582. To perform the transmission electron microscopy (TEM) analysis, specimens were prepared through mechanical grinding and twin jet electrolytic polishing in a 300ml HNO_3 + 700ml CH_3OH solution at -20^{0}C and a voltage of 20V. TEM micrographs were taken using a Philips CM200 transmission electron microscope operated at 200 kV. For EBSD analysis the surface of the sample was polished by electropolishing in a 100 ml $HClO_4$ + 900 ml CH_3OH solution at −20^{0}C

and a voltage of 50V. The EBSD measurements were carried out using the program TSL-OIM in a Philips XL30S SEM machine with a FE gun operated at 15 kV. The step size and scan area for EBSD mapping were chosen as 0.05μm and 20μm×20μm, respectively. X-ray diffraction measurement of the extruded aluminum billet and the aluminum layer was carried out on a Philips X pert Pro diffractometer with a Cu kα radiation between 20^o and 110^o using 0.01^o per 2 sec step size. The dislocation density was evaluated assuming a random distribution of dislocations[11, 12]:

$$\rho_{hkl} = \frac{2\sqrt{3}\left\langle \varepsilon^2{}_{hkl} \right\rangle^{1/2}}{D_{hkl} b} \tag{2}$$

where $<\varepsilon^2_{hkl}>^{1/2}$ is the microdistortion level, D_{hkl} the coherent domain size, and b is the Burgers vector.[11]

3. Results and Discussion

Fig. 2 exhibits that the yield stress of the deformed proof and of aluminum layer of the ECAE-ed laminated composite is significantly increased after one pass of ECAE, so that the yield stress becomes more than three times of the initial yield stress. However, the rate of increase in the yield stress in the subsequent passes is decreased substantially. Beyond the fourth pass, the yield stress of proof specimen is slightly decreased. Fig. 3 demonstrates the variation of dislocation density with number of ECAE passes. As it is seen dislocation density increases from 0.15×10^{14} to ~ 1.8×10^{14} in type II composite and to ~ $1.47\times10^{14} m^{-2}$ in proof specimen, respectively when the strain increases from 0 to about 4.3 (equivalent to four passes of ECAE). The dislocation densities are slightly decreased during further deformation of the composite and proof aluminum billets. Indeed, the yield strength is significantly increased due to the severe increase in dislocation density and possibly the initiation of production of smaller grains of high angle misorientation during the first two passes. However, after that the strain softening phenomenon is occurred due to dislocations rearrangement by increasing the number of ECAE passes up to 4. This phenomenon decreases the increasing rate of mobile dislocation density as a result of annihilation process, formation of locks, and the formation of dipoles.[13] On the other hand, with dislocation density variations, no appreciable reduction can be observed in the yield strength, even beyond 4 passes, by increasing the clad layer thickness (Fig. 2). This phenomenon is probably related to the strengthening compensation via grain boundary mechanism due to the continuous grain refinement. Fig. 4 shows the microstructure and the associated selected area electron diffraction (SAED) pattern of the proof specimen and type II composite after 2 passes of ECAE. As it is observed, the microstructure of aluminum strip located in the composite specimen consists of equiaxed ultrafine grains and poorly delineated grain boundaries

without interior dislocations, indicating a non-equilibrium state with fringed structure and high internal stress. This is justified as the rotation of the samples according to route Bc by $+90^0$, causes the shearing of deformed grain on two orthogonal planes in reverse direction. In other words, each individual shearing is reversed after the first shearing of the sample in the shearing planes, causing the division of the elongated grains and restoration of equiaxed grains. The mentioned phenomenon is confirmed by a set of ring selected area diffraction pattern presented in Fig. 4a. However, in the proof specimen (Fig. 4b), the dominant finding is the formation of a great amount of low energy dislocation structure (LEDS) with ill defined diffraction pattern. In route Bc, where different shear planes are used in consecutive passes, the grains can not maintain the stable orientation and consequently the HAB generation is more efficient via the texture

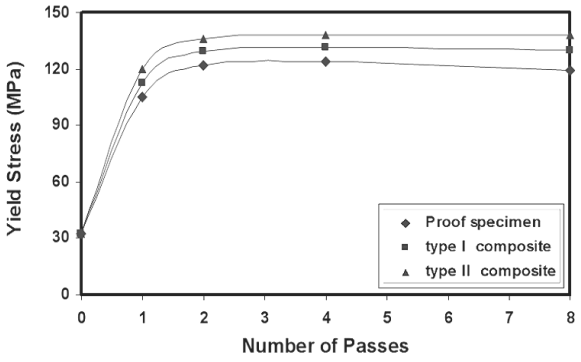

Fig. 2. Effect of the number of passes (equivalent to the amount of increase in deformation strain) on the yield stress of aluminum: proof and composite specimens.

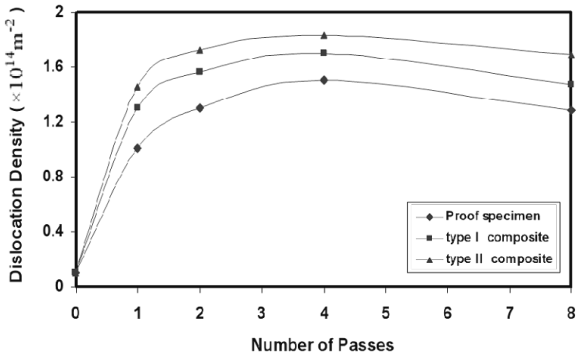

Fig. 3. Variations of dislocation density of aluminum layer with the number of passes: proof and composite specimens.

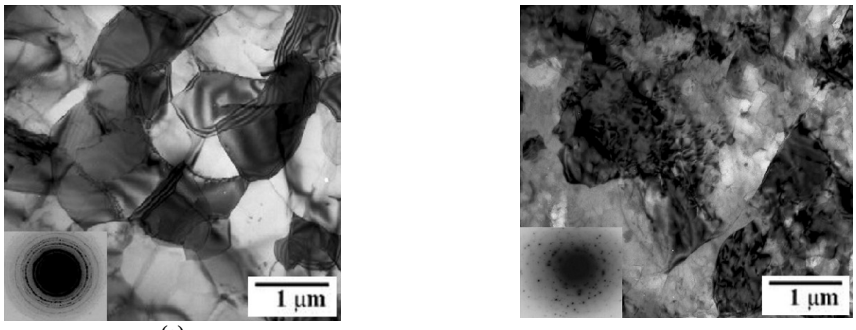

(a) (b)

Fig. 4. TEM micrographs and SAED pattern of aluminum: (a) type II composite and (b) proof specimen after 2 passes.

evolution mechanism.[14] Fig. 5 shows the orientation color maps taken from the aluminum layer of the laminated composite and the single billet after four passes. Referring to Fig. 5(a) the microstructure of aluminum proof specimen consists of elongated grains accompanied by a small quantity of equiaxed grains aligned with an angle which is nearly 45^0. In contrast, in the microstructure of the type II composite specimen the most of elongated grains appeared in the first passes are nearly broken into restored equiaxed grains (Fig. 5d). On the other hand, from the boundary maps in Figs. 5(b) and (e), it is obvious that the fraction of high angle grain boundaries in type II composite is larger than that of the proof specimen. In these figures the high angle grain boundaries with misorientation angle above 15^0 are shown as black lines, while the boundaries between 2^0 and 15^0 are shown as red lines. Also, Figs. 5(c) and (f) show the average distribution of misorientation angles. The average fraction of high angle grain boundaries and the average misorientation angle through the proof specimen section are 32.7% and 25.4^0, respectively (Fig. 5c). Whereas, in type II composite, the distribution is relatively different having two small peaks at medium and high angle misorientations and the average fraction of high angle grain boundaries and mean misorientation angle are 71.2% and 39.8^0, respectively (Fig. 5f). The bimodal misorientation distribution is the characteristic of the SPD- processed ultrafine grain materials.[15]

Table 1 summarizes the results of the EBSD and TEM measurements obtained from the proof and composite specimens subjected to 1, 4, and 8 passes. It is seen that the mean (sub)grain size value from the TEM studies are smaller than those measured from EBSD analysis. This arises from the fact that the boundaries with misorientation angle below 2^0 are visible in TEM microstructures, which subdivide the grains into the smaller units. Also, this table shows the fraction of HAGB is significantly increased by increase in number of passes and thickness of copper cladding layers. Moreover, at a constant number of pass the HAGBs area fraction is larger in the composite specimens compared

with that of proof specimen. It is seen that there are no increases in dislocation density between 4 and 8 passes (Fig. 3). However, at the same time, based on the results presented in Table 1, the grain orientation distribution changes even between 4 and 8 passes and persists the grain refinement. Thereby, a large fraction of the grains is refined to ultrafine size at the first two passes of composite specimen. As it is clearly evident in

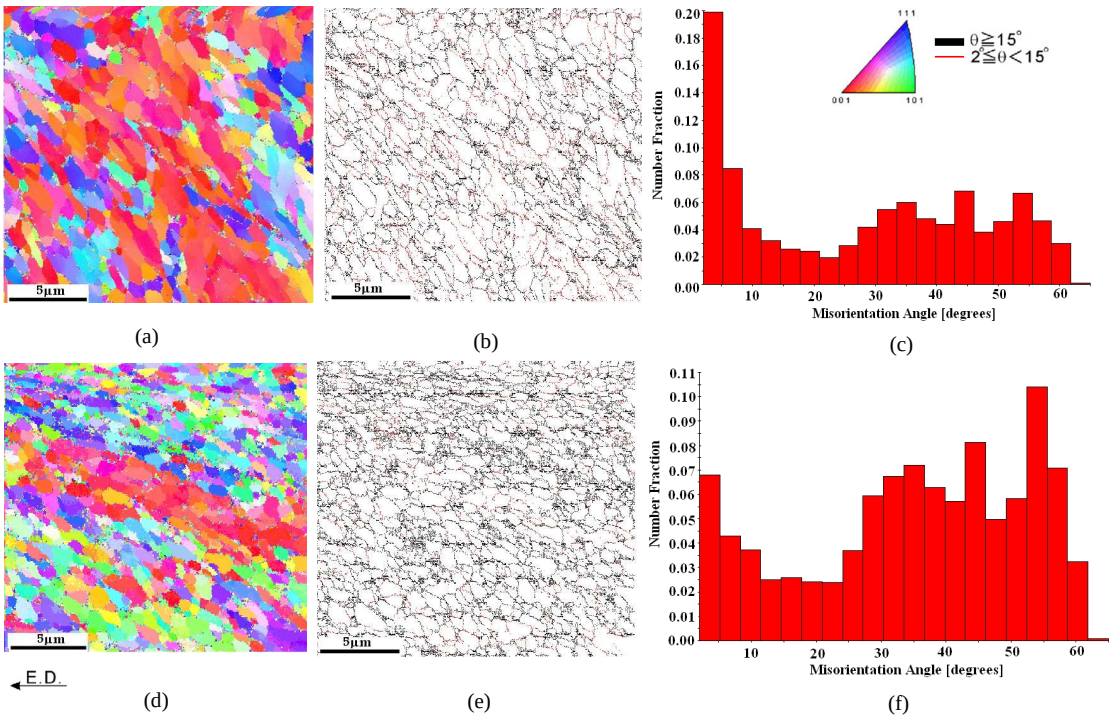

Fig. 5. The color maps, boundary maps, and distribution of the boundary misorientation angles obtained from the EBSD data of the ECAE throughout 4 passes, (a, b, and c) proof specimen and (d, e, and f) type II composite.

Table. 1. Microstructural parameters measured in different specimens from TEM and EBSD analyses.

Number of passes applied	Average cell size (nm) determined by TEM technique			Average cell size (nm) determined by EBSD analysis			HAGBs area fraction (%) determined by EBSD analysis		
	proof specimen	type I composite	type II composite	proof specimen	type I composite	type II composite	proof specimen	type I composite	type II composite
1	1450	1200	870	2850	2300	1660	21.5	42.4	50.3
4	1100	900	750	2900	1700	1330	32.7	59.5	71.2
8	910	880	550	1740	1630	990	39.8	65.3	78.5

Fig. 6, the (111) pole figures exhibit the change in microstructure of type II composite compared to that of the proof specimen subjected to 2 ECAE passes from an initial shear texture (Fig. 6a). As it is seen, the texture of proof specimen represents a close to ideal shear texture (Fig. 6b), whereas the type II composite specimen, Fig. 6c, shows evidence of deviation from ideal shear texture (i.e., B component). This shift might be due to deformation state, strain hardening and friction condition.[16]

Thus, one may suggest that the deformation mode of the aluminum layer in composite has altered to some extent compared with the single billet. Moreover, Beyerlin et al.[17] has reported that the shape of grains affects the textural evolution. Therefore, it is anticipated that the texture of composite specimen with equiaxed microstructure is different from that of proof specimen with grains of higher average aspect ratio. Likewise, further passes (N=4) have led to a weakening of all ideal shear type orientation (e.g., C_0 and A^*_{10}) (Fig. 6d). On the other hand, the re-appearance of weak texture components of the initial texture reflects glide-reversal effects that return part of the substructure into an equiaxed configuration. The interpretation of the pole figures can be made with the aid of a key pole figure with the locations of the ideal ECAE orientations given by Dalla Torre et al.[18]

Worth mentioning that the new high angle boundaries (HABs) generation in cold worked metals are mainly caused by two mechanisms: microstructural mechanism and texture mechanism.[19] According to the microstructural mechanism, original grains are subdivided by dislocation boundaries, and the misorientation angles associated with them are increased with increasing strain. HABs generated by this mechanism are expected to produce boundaries with misorientation angles mainly up to 15^0–30^0. The texture mechanism involves grain subdivision by cell blocks and the rotation of the subdivided grains to different preferred textures during deformation. HABs formed by this mechanism are often of wide range of misorientation angles, 20^0–60^0.[14] The operation of these two mechanisms basically depends on the grain orientation, strain, and deformation mode.[19] Regarding the mentioned phenomena, one can conclude that the yield strength and the HAGBs area fraction are raised by the increase in number of ECAE passes and thickness of copper clad layers. Indeed, placing softer aluminum strip between two hard

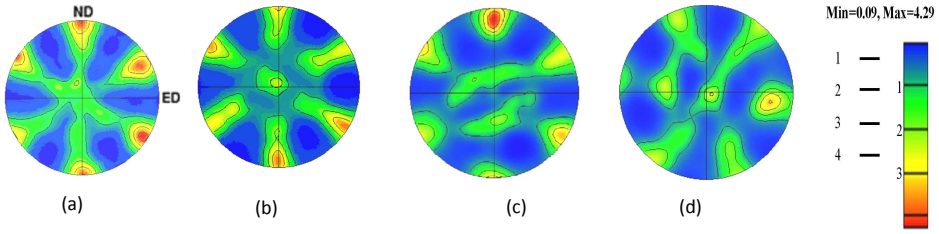

Fig. 6. (111) pole figures (a, b) for proof specimen after one and two passes, (c, d) for type II composite after two and four passes, respectively. Countor levels: 0.5×

copper strips may lead to further refinement in the middle layer due to additional normal stress from the copper layers. The aluminum layer is prevented to flow by means of the copper layer. This constraint acts as a back pressure.[20] Accordingly, the operative slip systems may be affected on a microscopic level and hence the resulting texture and further grain refinement. Clearly, this assessment involves the application of FEM simulation to evaluate the deformation behavior of each layer. For the sake of brevity it is not possible to present the FEM results in this paper. They will be presented elsewhere.

4. Conclusions

In this research, the loosely packed tri-layer copper-aluminum-copper laminated composites were ECA-extruded and the yield strength, the grain size, and the misorientation of grain boundaries of the aluminum layer were evaluated and compared with those of a mono layer aluminum billet ECA-extruded at the same conditions of the laminated composite. The aim was to improve the grain refinement in commercial pure aluminum produced so far using ECAE process and to accelerate it. The following conclusions can be drawn from the achieved results:

(1) The ECAE process increases the aluminum yield strength up to four times and the rate of increase in strength is significantly decreased after the first pass and becomes insignificant or weak after the fourth pass.
(2) The grain size of the aluminum layers in Cu-Al-Cu deformed by ECAE process is decreased by increasing the thickness of the copper cladding layers.
(3) The rate of grain refinement in the aluminum layer of the composite is increased by increasing the strain of ECAE process due to microstructural mechanism up to fourth pass and thereafter the textural evolution is responsible.
(4) The HAGB area fraction is enhanced by increasing the copper cladding thickness during the subsequent ECAE passes. In other words, due to variation of deformation behavior a finer grain size can be achieved at a smaller number of passes in an aluminum strip by sandwiching it between two Cu strips and then extruding the sandwich billet.

Acknowledgements

The authors would like to thank the Iran National Science Foundation (INSF) and Research Board of Sharif University of Technology, Tehran, Iran, for the financial support and provision of the research facilities used in this work. They also thank Dr. Erhard Schafler at Physics of Nanostructured Materials, Faculty of Physics, University of Vienna, Austria for preparing the EBSD results and the useful discussion.

References

1. H. C. Kwon, T. K. Jung, S. C. Lim and M. S. Kim, Mater. Sci. Forum. **449-452**, 317 (2004).
2. J. Ziegelheim, S. Hiraki, H. Ohsawa, Jour. Mater. Process. Technol. **186**, 87 (2007).
3. B. Gulenc, Mater. & Design. **29**, 275 (2007).
4. B. Tolaminejad, H. Arabi, Iranian Jour. of Sci. Technol., Trans. B, Eng. **32(B6)**, 631 (2008).
5. M. Shaarbaf, M. R. Toroghinejad, Mater. Sci. Eng. A. **473**, 28 (2008).
6. V. M. Segal, Mater. Sci. Eng. A. **197**, 157 (1995).
7. Y. Iwahashi, J. Wang, Z. Horita, M. Nemoto and T. G. Langdon, Scripta Mater. **35**, 143 (1996).
8. A. R. Eivani, A. Karimi Taheri, Mater. Lett. **61**, 4110 (2007).
9. V. I. Kopylov, V. N. Chuvildeev, in Ultra grain refinement by ECAP: experiment and theory - Proc. Ukraine Int. Symp. on Nanostructured materials by High-pressure severe plastic deformation, ed. D. Orlov et al. (Nato advanced study institute, 2006), pp.69.
10. R. Z. Valiev, T. G. Langdon, Prog. Mater. Sci. **51**, 881 (2006).
11. N. A. Enikeev, H. S. Kim, I. V. Alexandrov, Mater. Sci. Eng. A. **460–461**, 619 (2007).
12. W. Pantleon, Mater. Sci. Eng. A. **400-401**, 118 (2005).
13. M. Goerdeler, G. Gottstein, Mater. Sci. Eng. A. **309–310**, 377 (2001).
14. P. L. Sun, P. W. Kao, C. P. Chang, Scripta Mater. **51**, 565 (2004).
15. X. Huang, N. Tsuji, N. Hansen, Y. Minamino, Mater. Sci. Eng.A. **340**, 265 (2003).
16. X. Molodova , G. Gottstein , M. Winning , R.J. Hellmig, Mater. Sci. Eng. A. **460–461**, 204 (2007).
17. I. J. Beyerlein, L. S. Tóth, Prog. Mater. Sci. **54**, 427 (2009).
18. F. H. Dalla Torre, A. A. Gazder, E.V. Perloma and C. H. J. Davies, Jour. Mater. Sci. **43**, 3364 (2007).
19. D. A. Hughes, N. Hansen, Acta Mater. **45**, 3871 (1997).
20. R. K. Oruganti, P. R. Subramanian, J. S. Marte, M. F. Gigliotti and S. Amancherrla, Mater. Sci. Eng. A. **406**, 102 (2005).